Slipping instability in a system of two superposed fluid layers

Chiara Toniolo

1 Introduction

The stability of the interface between two layers of immiscible, incompressible fluids is studied. Since the fluids may have distinct physical properties, the interface is susceptible to instabilities due to density stratification, shear-flow instabilities or interfacial ones, arising from discontinuities in longitudinal stresses at the boundary between the two media ([14], [15], [4], [13]).

The motivation of this analysis is the study of a particular kind of fast flowing glacier, found in the Antartica and in Greenland and known with the name of *ice stream*. An ice stream can be generically identified, as a part of an inland ice sheet that flows rapidly through the surrounding ice ([10]). Ice streams appear as long, shallow tongues, extended in the two horizontal directions and may end as outlet glaciers, bordered by rocks, or as ice shelves, floating over water. Altough they represent only a low percentage of the Antarctic coastline, they may drain out of the polar regions a substancial part of the accumulation in the interior.

Since ice stream motion provides a process for rapid dispersal and disintegration of ice sheets, an understanding of the underlying physical mechanism of ice streaming flow is, other than intriguing by itself, relevant in attempting to evaluate the dynamics of continental expanses.

In order to explain the basic mechanisms of the instability is necessary to explore the physical properties of the till, the layer at the bottom of these fast moving streams. The till is a complex material consisting of a liquid, deformable, inhomogeneous, anisotropic mixture of water and unconsolidated sediments ([5]). As a consequence of the high pressures, the base of the stream is often melted rather than frozen.

All the existing quantitative models of ice stream dynamic thus relate the characteristics of the flow to the complex nature of the basal layer and to the interactions between the latter and the thick overlying frozen one.

In general, four different kind of explanations of ice-stream behaviour are usually found in literature:

- sliding of the thick ice layer over the thin till, acting as a lubricant ([8], [9]);
- shear deformation of the water-saturated till underlying the ice ([1]);

- thermomechanical feedback, arising from the dependence of viscosity on temperature of ice ([11], [12]);
- superplasticity of the till ([7]).

What follows will be concerned with the first two mechanical interpretations of ice stream dynamic. The aim of this work is the investigation of the peculiar properties of such a kind of flow, considered as a mechanism resulting from the combination of glacier-like sliding and ice-shelf slipping.

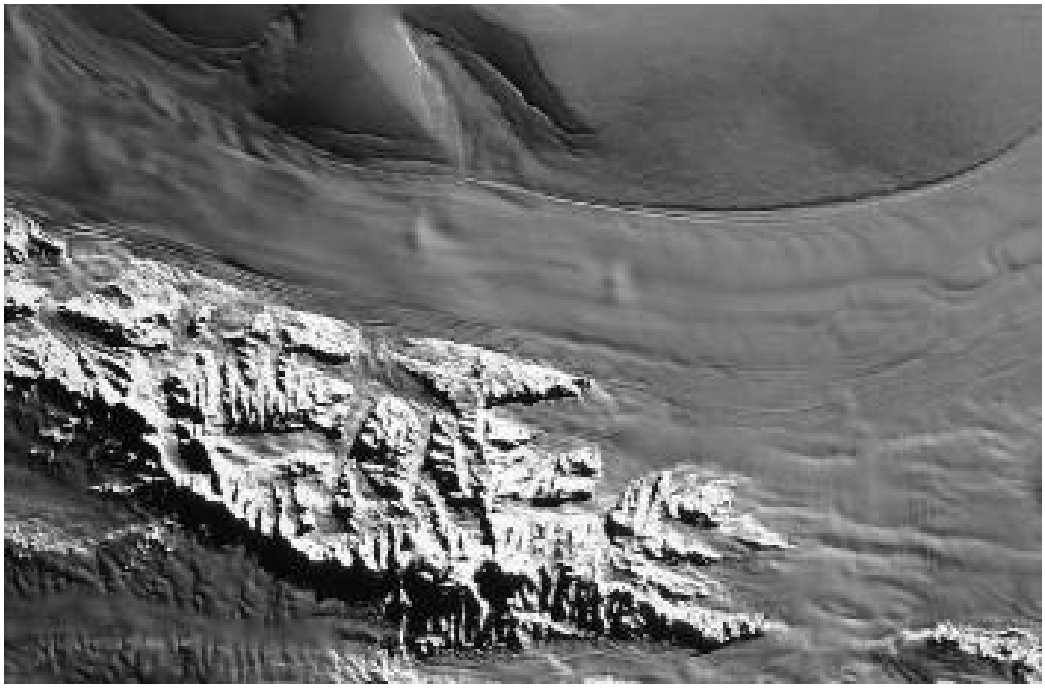

Figure 1: Landsat image of Rutford Ice Stream B, West Antartica, flowing from left to right between the solid rock wall on one side and low lying ice-covered promontory on the other. Image courtesy of D. D. Blankenship et al., Geophysical and Polar research Center, University of Wisconsin-Madison.

In the past, several models of fast sliding glaciers have been applied to ice-streams, most of them having included semiempirical laws to express the stress at the bottom of the mass of ice. This trick allows to simplify the mathematics, since an explicit formulation of the basal dynamic is not required, but in some way it introduces arbitrary assumptions in the formulations.

In the commonly accepted interpretation, the glacier is sliding on a deforming bed, usually a frozen one, absorbing most or all of the differential motion between the ice and the bedrock. On the other hand an ice-shelf spreading is due to longitudinal, rather than

shear stresses, which its floating base cannot support. Given these, there is a deep dynamic difference between a fast moving glacier and an ice-shelf.

To the discussion about the governing equations, the derivations of the glacier and ice-shelf models and a preliminary stability analysis will follow. Finally, a one-dimensional ice-stream model will be introduced.

2 Mathematical Formulation

Since the key ingredient in the fast stream dynamic is the interaction between the till and the ice over it, in order to limit as much as possible the amount of assumptions on the structure of the stresses regarding the till, all the models presented hereafter will be two layer ones.

2.1 Basic equations

The evolution of a flow with longitudinal and transversal structure is described by a set of three dimensional, non steady, isothermal equations.

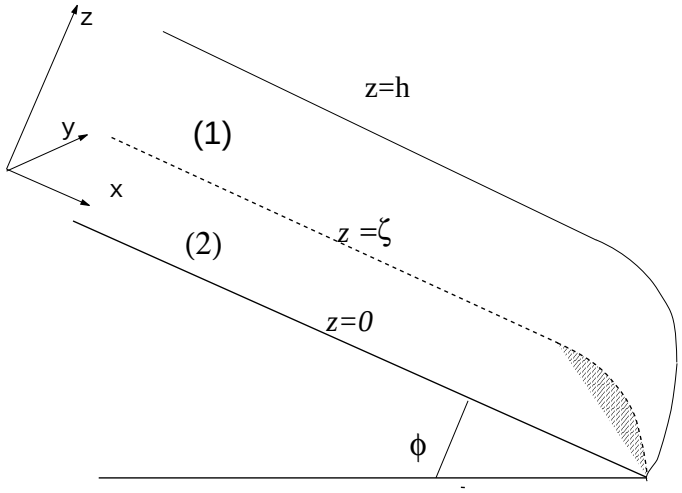

Figure 2: The coordinate system and the configuration for the two fluids

In the continuum hypothesis, having decoupled the dynamic problem from the thermodynamic one, the governing equations for the two fluids reduce to the incompressible continuity equation and to the conservation of momentum. Defined an orthogonal coordinate system as in figure (2), z being the vertical coordinate and $S = tan(\phi)$ the slope of the fixed bottom, the equations representing the two layers are:

$$\begin{aligned} u_{1x} + v_{1y} + w_{1z} &= 0 \\ u_{1t} + uu_{1x} + vu_{1y} + wu_{1z} &= -\frac{1}{\rho_1} p_{1x} + \frac{1}{\rho_1}(\partial_x \tau_{xx} + \partial_y \tau_{xy} + \partial \tau_{xz}) + g sin(\phi) \end{aligned}$$

$$
\begin{aligned}
v_{1t} + uv_{1x} + vv_{1y} + wv_{1z} &= -\frac{1}{\rho_1}p_{1y} + \frac{1}{\rho_1}(\partial_x\tau_{xy} + \partial_y\tau_{yy} + \partial_z\tau_{yz}) \\
w_{1t} + uw_{1x} + vw_{1y} + ww_{1z} &= -\frac{1}{\rho_1}p_{1z} + \frac{1}{\rho_1}(\partial_x\tau_{xz} + \partial_y\tau_{yz} + \partial_z\tau_{zz}) - gcos(\phi) \qquad (1)
\end{aligned}
$$

and:

$$
\begin{aligned}
u_{2x} + v_{2y} + w_{2z} &= 0 \\
u_{2t} + uu_{2x} + vu_{2y} + wu_{2z} &= -\frac{1}{\rho_2}p_{2x} + \frac{1}{\rho_2}(\partial_x\sigma_{xx} + \partial_y\sigma_{xy} + \partial\sigma_{xz}) + gsin(\phi) \\
v_{2t} + uv_{2x} + vv_{2y} + wv_{2z} &= -\frac{1}{\rho_2}p_{2y} + \frac{1}{\rho_2}(\partial_x\sigma_{xy} + \partial_y\sigma_{yy} + \partial_z\sigma_{yz}) \\
w_{2t} + uw_{2x} + vw_{2y} + ww_{2z} &= -\frac{1}{\rho_2}p_{2z} + \frac{1}{\rho_2}(\partial_x\sigma_{xz} + \partial_y\sigma_{yz} + \partial_z\sigma_{zz}) - gcos(\phi) \qquad (2)
\end{aligned}
$$

where the subscripts (x,y,z) denote partial derivatives, (1) and (2) refer to the upper and lower fluid, $\mathbf{u} = (u, v, w)$ is the velocity field, $\mathbf{g} = (gsin(\phi), 0, -gcos(\phi))$ is the gravity force, τ_{ij} and σ_{ij} the anisotropic parts of the stress tensors, the total deviatoric tensors being respectively:

$$
\begin{aligned}
\mathbb{T} &= \tau - p_1\mathbb{I} \\
\mathbb{S} &= \sigma - p_2\mathbb{I} \qquad (3)
\end{aligned}
$$

2.2 Boundary conditions

The problem needs, to be defined, the specification of the associated boundary conditions.

At the base of the stream a no-slip condition is required. Since the base is kept fixed, this imposes on z=0:

$$u_2 = v_2 = w_2 = 0 \qquad (4)$$

At the interface $z = \zeta$ between the two media the physical request of matching of the stresses has to be satisfied:

$$\mathbb{T} \cdot \mathbf{n}_\zeta = \mathbb{S} \cdot \mathbf{n}_\zeta \qquad (5)$$

having defined $\mathbf{n}_\zeta = (-n_x, -n_y, 1)/(n_x^2 + n_y^2 + 1)$ as the unit normal pointing out of the surface $z = \zeta$.

The last one at the free surface imposes a zero stress at the elevation $z = h$:

$$\mathbb{T} \cdot \mathbf{n}_h = \mathbf{0} \qquad (6)$$

and expresses the continuity of stresses between the upper layer and a medium (air) much less dense overlying it.

2.3 Rheology of the problem

The system is then closed specifying the functional relation between the stress tensors $\mathbb{T}$ and $\mathbb{S}$ and the properties of the two fluids. This defines the analogous of the Newtonian constant viscosity in the case of a nonlinear relationship between strain rate and stress.

A fairly general model is a power law contitutive relation of the kind:

$$\tau_{ij} = K\dot{\gamma}^{n-1} \cdot \dot{\gamma}_{ij} \tag{7}$$

where K is the consistency, dependent on temperature, pressure, composition of the material, $n > 0$ a fixed real exponent ($n = 1$ for a Newtonian fluid) and $\dot{\gamma}$ the second invariant of the strain rate, expressed by:

$$\dot{\gamma} = \sqrt{\frac{1}{2}\dot{\gamma}_{jk} \cdot \dot{\gamma}_{jk}} \tag{8}$$

According to the previous notation, the strain rate tensor becomes:

$$\dot{\gamma}_{ij} = \begin{pmatrix} 2u_x & u_y + v_x & u_z + w_x \\ u_y + v_x & 2v_y & v_z + w_y \\ u_z + w_x & v_z + w_y & 2w_z \end{pmatrix} \tag{9}$$

In the till-ice system, none of the two components has a simple behaviour. Nonetheless, a proper discussion of the rheological properties of the till goes beyond the aim of this work and could eventually follow to a first understanding of the primary instability mechanism.

In the model presented further on, the till will be considered like a Newtonian fluid, with constant viscosity, while for ice the constitutive relation will be a power law one of the kind discussed above (7). Ice is a shear thinning fluid, in the sense that an increased strain rate produces a decrease in the effective viscosity. In fact, for ice:

$$n \sim \frac{1}{3} \tag{10}$$

The equation (7) is in this case (and for all values of $n < 1$), not well behaved for some particular flow configuration, predicting in fact an infinite effective viscosity for values of the strain rate approaching zero.

3 The Glacier Theory

In a glacier the slab deformation at a generic depth is moslty due to shear stress, the bottom attached to the rock being commonly frozen.

Thus the minimum model for such a kind of system is represented by the superposition of two Newtonian fluids with different densities and viscosities, described at leading order by an hydrostatic balance in the vertical and by a balance between pressure gradient force and shear stress in the horizontal direction x.

3.1 Non-dimensional equations

Focusing the attention on the one-dimensional case, the relevant balance in the x-momentum equation is expressed for both fluids by:

$$p_{1x} \sim \partial_z \tau_{xz} \tag{11}$$

$$p_{2x} \sim \partial_z \sigma_{xz} \tag{12}$$

Continuity and momentum conservation equation reduce, in a one-dimensional framework, to:

$$\begin{aligned} u_{1x} + w_{1z} &= 0 \\ u_{1t} + u_1 u_{1x} + w u_{1z} &= -\frac{1}{\rho_1}\partial_x p_1 - \frac{1}{\rho_1}(\partial_x \tau_{xx} + \partial_z \tau_{xz}) + g sin\phi \\ w_{1t} + u_1 w_{1x} + w w_{1z} &= -\frac{1}{\rho_1}\partial_z p_1 - \frac{1}{\rho_1}(\partial_x \tau_{xz} + \partial_z \tau_{zz}) - g cos\phi \end{aligned} \tag{13}$$

$$\begin{aligned} u_{2x} + w_{2z} &= 0 \\ u_{2t} + u_2 u_{2x} + w u_{2z} &= -\frac{1}{\rho_2}\partial_x p_2 - \frac{1}{\rho_2}(\partial_x \sigma_{xx} + \partial_z \sigma_{xz}) + g sin\phi \\ w_{2t} + u_2 w_{2x} + w w_{2z} &= -\frac{1}{\rho_2}\partial_z p_2 - \frac{1}{\rho_2}(\partial_x \sigma_{xz} + \partial_z \sigma_{zz}) - g cos\phi \end{aligned} \tag{14}$$

where the subscripts 1 and 2 refer to the upper and lower fluid respectively.

The set of equations above is then non dimensionalized by choosing the following scales:

$$x = L\tilde{x},\ z = H\tilde{z},\ u = U\tilde{u},\ w = \frac{UH}{L}\tilde{w},\ t = \frac{L}{U}\tilde{t} \tag{15}$$

For pressure:

$$p = \rho_1 g H \tilde{p} \tag{16}$$

and strain rate:

$$\dot{\gamma}_{ij} = \frac{U}{H}\tilde{\dot{\gamma}}_{ij} \tag{17}$$

The leading order balance defines then the scale for horizontal velocity $U = \frac{\rho_1 g H^3}{\nu_1 L}$. With this restriction, defining as $\epsilon = \frac{H}{L}$ the aspect ratio for the two thin layers and indicating with $Re = \frac{\rho_1 U L}{\nu_1}$ the small Reynolds number of the flow, the inertial terms in the governing equations become negligible at leading orders, being proportional to $\epsilon^2 Re$.

The simplified non dimensional form of the governing equations, dropping the tilde superscript, is then:

$$\begin{aligned} 0 &= u_{1x} + w_{1z} \\ 0 &= -p_{1x} + \epsilon \partial_x \tau_{xx} + \partial_z \tau_{xz} + S \\ 0 &= -p_{1z} + \epsilon^2 \partial_x \tau_{xz} + \epsilon \partial_z \tau_{zz} - 1 \end{aligned} \tag{18}$$

$$\begin{aligned} 0 &= u_{2x} + w_{2z} \\ 0 &= -p_{2x} + \epsilon \partial_x \sigma_{xx} + \partial_z \sigma_{xz} + SD \\ 0 &= -p_{2z} + \epsilon^2 \partial_x \sigma_{xz} + \epsilon \partial_z \sigma_{zz} - D \end{aligned} \tag{19}$$

where $S = \frac{tan\phi L}{H}$ is the non dimensional slope and $D = \frac{\rho_2}{\rho_1}$ is the density ratio. The components of the strain rate tensor, in the new rescaled variables are:

$$\dot{\gamma}^{(i)}_{xx} = 2\epsilon u_{ix} \qquad \dot{\gamma}^{(i)}_{xz} = u_{iz} + \epsilon^2 w_{ix} \qquad \dot{\gamma}^{(i)}_{zz} = 2\epsilon w_{iz} \tag{20}$$

where i=1,2.

The system is finally defined by the boundary conditions at the rigid bottom boundary $z = 0$:

$$u_2 = w_2 = 0 \tag{21}$$

at the interface $z = \zeta$ between the two fluids:

$$\begin{aligned} -\epsilon(\tau_{xx} - p_1)\zeta_x + \tau_{xz} &= -\epsilon(\sigma_{xx} - p_2)\zeta_x + \sigma_{xz} && (22)\\ -\epsilon\tau_{xz}\zeta_x + (\tau_{zz} - p_1) &= -\epsilon\sigma_{xz}\zeta_x + (\sigma_{zz} - p_2) && (23)\\ & && (24) \end{aligned}$$

and at the free surface $z = h$:

$$\begin{aligned} -\epsilon(\tau_{xx} - p_1)\zeta_x + \tau_{xz} &= 0 && (25)\\ -\epsilon\tau_{xz}\zeta_x + (\tau_{zz} - p_1) &= 0 && (26) \end{aligned}$$

3.2 The 1-D thin glacier theory

The derivation of a thin layer model ([2], [3]) describing the evolution of the system at the boundaries, follows directly from the assumption of a shallow layer for both ice and till.

The smallness of the aspect ratio ϵ allows to perform an asymptotic expansion of the governing equations, reducing the complexity of the initial formulation to a simplified set of equations that incorporate the basic physical aspects of the phenomenon.

This is done by expanding all the variables in power series of ϵ:

$$u_i = u_i^{(0)} + \epsilon u_i^{(1)} + O(\epsilon^2), w_i = w_i^{(0)} + \epsilon w_i^{(1)} + O(\epsilon^2), p_i = p_i^{(0)} + \epsilon p_i^{(1)} + O(\epsilon^2) \quad \cdots \tag{27}$$

and so on. Collecting terms of the same order in ϵ one obtain a set of governing equations that solves the problem at the different orders.

At leading order, according to the previous definition (20) of the strain rate tensor:

$$\tau_{zz}^{(0)} = -\tau_{xx}^{(0)} = 0 \tag{28}$$

and seemingly:

$$\sigma_{zz}^{(0)} = -\sigma_{xx}^{(0)} = 0 \tag{29}$$

indicating a basic flow independent on z in the upper layer.

The interior flow is thus completely determined specifying the velocity field (u, w) at the boudaries and solving the two evolution equations for ζ and h:

$$\begin{aligned} \zeta_t + u(\zeta)\zeta_x &= w(\zeta) && (30)\\ h_t + u(h)h_x &= w(h) && (31) \end{aligned}$$

The pressure field, hydrostatic at leading order, is given by:

$$p_1^{(0)} = h - z \tag{32}$$

and

$$p_2^{(0)} = h - \zeta + D(\zeta - z) \tag{33}$$

(the (0) superscript at the right end side of the equations have been dropped for convenience).

Then, integrating the second of (18) along the vertical and given the upper boundary condition $\tau_{xz}^{(0)}(h) = 0$:

$$\sigma_{xz}(\zeta) = (S - h_x)(h - \zeta) \tag{34}$$

Here, the stress component σ_{xz} is evaluated from an integration in the lower layer:

$$\sigma_{xz}^{(0)}(\zeta) = (\zeta - z)(h_x - \zeta_x + D\zeta_x - SD) + \sigma_{xz}(z) \tag{35}$$

The velocity at the boundary $z = \zeta$, equating (34) and (35) is:

$$u = \frac{1}{\nu_2}[(S - h_x)(h - \zeta)\zeta - (h_x - \zeta_x + D\zeta_x - SD)\frac{\zeta^2}{2}] \tag{36}$$

Since at leading order the flow is independent on z:

$$u(h) = u(\zeta) \tag{37}$$

while for the vertical component of velocity (integration of continuity equation):

$$w(h) = w(\zeta) - \int_{\zeta}^{h} u_x dz = w(\zeta) - u_x(\zeta)(h - \zeta) \tag{38}$$

The final set of equations, defining $\theta = h - \zeta$ to be the thickness of the upper layer is then:

$$\zeta_t + \partial_x[(S - h_x)\frac{\theta\zeta^2}{2} + (\theta_x + D\zeta_x - DS)\frac{\zeta^3}{3}] = 0 \tag{39}$$

$$R\theta_t + \partial_x[(S - h_x)\frac{\theta^3}{3} + \theta u] = 0 \tag{40}$$

$$u = R[\frac{\zeta^2}{2}(DS - D\zeta_x - \theta_x) + (S - h_x)\theta\zeta] \tag{41}$$

where the new relevant parameter R is a viscosity ratio of the form $\frac{\nu_1}{\nu_2}$.

3.3 The 2-D extension

It's straightforward the generalization in presence of a bidimensional horizontal structure:

$$u - R[(S - h_x)\theta\zeta + \frac{\zeta^2}{2}(DS - D\zeta_x - \theta_x)] = 0$$

$$v + R[h_y\theta\zeta + \frac{\zeta^2}{2}(D\zeta_y + \theta_y)] = 0$$

$$R\theta_t + \partial_x[(S - h_x)\frac{\theta^3}{3} + \theta u] + \partial_y[-h_y\frac{\theta^3}{3} + \theta v] = 0$$

$$\zeta_t + \partial_x(S - h_x)\frac{\theta\zeta^2}{2} - (\theta_x + D\zeta_x - DS)\frac{\zeta^3}{3}] - \partial_y[h_y\frac{\theta\zeta^2}{2} + (\theta_y + D\zeta_y)\frac{\zeta^3}{3}] = 0 \tag{42}$$

here (u,v) indicate the velocity components in the directions (x,y).

4 The Ice-Shelf Theory

In a ice-shelf, floating on the sea, the lower layer is liquid water, much less viscous than the ice moving on it. In this case, considering pretty uniform the thickness of the shallow layer of ice, the vertical shear is zero and the big mass of ice behaves like a uniform slab, subject to zero fricton at its upper and lower surfaces.

4.1 Non-dimensional equations

In the 1-D model, the essential balances for the two fluids are expressed by:

$$p_{1x} \sim \partial_x \tau_{xx} \tag{43}$$

$$p_{2x} \sim \partial_x \tau_{xz} \tag{44}$$

From equation (43) it's clear the relevance of the longitudinal stresses in the ice layer.

The set of equations (13), (14) is again non-dimensionalized using the same scales as for the glacier case, getting:

$$\begin{aligned} 0 &= u_{1x} + w_{1z} \\ 0 &= -\epsilon p_{1x} + \epsilon \partial_x \tau_{xx} + \partial_z \tau_{xz} + S \\ 0 &= -p_{1z} + \epsilon \partial_x \tau_{xz} + \partial_z \tau_{zz} - 1 \end{aligned} \tag{45}$$

and:

$$\begin{aligned} 0 &= u_{2x} + w_{2z} \\ 0 &= -p_{2x} + \epsilon \partial_x \sigma_{xx} + \partial_z \sigma_{xz} + SD \\ 0 &= -p_{2z} + \epsilon^2 \partial_x \sigma_{xz} + \epsilon \partial_z \sigma_{zz} - D \end{aligned} \tag{46}$$

where the components of the strain rate tensors are respectively:

$$\dot{\gamma}^{(1)}_{xx} = 2u_{1x} \qquad \dot{\gamma}^{(1)}_{xz} = \frac{1}{\epsilon} u_{1z} + \epsilon w_{1x} \qquad \dot{\gamma}^{(1)}_{zz} = 2w_{1z} \tag{47}$$

and:

$$\dot{\gamma}^{(2)}_{xx} = 2\epsilon u_{2x} \qquad \dot{\gamma}^{(2)}_{xz} = u_{2z} + \epsilon^2 w_{2x} \qquad \dot{\gamma}^{(2)}_{zz} = 2\epsilon w_{2z} \tag{48}$$

It's worth noting how the stress components are defined and scaled differently in the two layers. In fact, for the upper fluid:

$$[p_1] = [p] = [\tau_{ij}] \tag{49}$$

while for the lower one:

$$[p_2] = [p] = \frac{1}{\epsilon} [\sigma_{ij}] \tag{50}$$

and from the continuity of pressures at the boundary $z = \zeta$ between the two media:

$$[\sigma_{ij}] = \epsilon [\tau_{ij}] \tag{51}$$

In the case of two Newtonian fluids, remembering the definitions given above for the components of the strain rate:

$$\frac{[\tau_{ij}]}{[\sigma_{ij}]} = \frac{\nu_1}{\nu_2} = R = \epsilon^{-2} \tag{52}$$

The boundary conditions at the rigid bottom z=0:

$$u_2 = w_2 = 0 \tag{53}$$

at level $z = \zeta$:

$$\begin{aligned} -\epsilon\zeta_x(\tau_{xx} - p_1) + \tau_{xz} &= -\epsilon\zeta_x(\epsilon\sigma_{xx} - p_2) + \epsilon\sigma_{xz} && (54)\\ -\epsilon\zeta_x\tau_{xz} + \tau_{zz} - p_1 &= -\epsilon\zeta_x\epsilon\sigma_{xz} + \epsilon\sigma_{zz} - p_2 && (55) \end{aligned}$$

and at the free surface $z = h$:

$$\begin{aligned} -\epsilon h_x(\tau_{xx} - p_1) + \tau_{xz} &= 0 && (56)\\ -\epsilon h_x\tau_{xz} + \tau_{zz} - p_1 &= 0 && (57) \end{aligned}$$

finally close the problem.

4.2 The thin ice-shelf theory

With a procedure completely similar to the one followed in section (3.2) one can obtain the evolution equations for the two boundaries $z = \zeta$, $\theta = h - \zeta$ and for the velocity u in a 1-dimensional framework:

$$\begin{aligned} R[\theta(2\tau_{xx})]_x - (\theta_x + \zeta_x - S)\theta - \frac{u}{\zeta} - \frac{\zeta}{2}(\theta_x + D\zeta_x - DS) &= 0\\ \theta_t + (u\theta)_x &= 0\\ \zeta_t + (\frac{u\zeta}{2})_x - \frac{1}{12}[\zeta^3(\theta_x + D\zeta_x - DS)]_x &= 0 \end{aligned} \tag{58}$$

and in the 2-dimensional one:

$$\begin{aligned} R([\theta(2\tau_{xx} + \tau_{yy})]_x + [\theta\tau_{xy}]_y) - (\theta_x + \zeta_x - S)\theta - \frac{u}{\zeta} - \frac{\zeta}{2}(\theta_x + D\zeta_x - DS) &= 0\\ R([\theta(\tau_{xx} + 2\tau_{yy})]_y + [\theta\tau_{xy}]_x) - (\theta_y + \zeta_y)\theta - \frac{v}{\zeta} - \frac{\zeta}{2}(\theta_y + D\zeta_y) &= 0\\ \theta_t + (u\theta)_x + (v\theta)_y &= 0\\ \zeta_t + (\frac{u\zeta}{2})_x + (\frac{v\zeta}{2})_y - \frac{1}{12}[\zeta^3(\theta_x + D\zeta_x - DS)]_x - \frac{1}{12}[\zeta^3(\theta_y + D\zeta_y)]_y &= 0 \end{aligned} \tag{59}$$

with the usual meaning of the parameters R, D and S involved.

5 Stability analysis

5.1 Linear stability

The first step in the understanding of the instability mechanism is to perform a linear stability analysis of the two systems presented, in a drastically simplified configuration of two Newtonian superposed fluids, perturbing around a basic state independent on the transversal coordinate y and uniform along the longitudinal x-direction.

One of the aims of this kind of study is to look for the occurrence of fingering instabilities in the horizontal plane.

The parameters determining the stability properties are:

- the non-dimensional slope S;
- the density ratio D ($=\rho_2/\rho_1$);
- the viscosity ratio R ($=\nu_1/\nu_2$);
- the scale of the upper layer thickness Θ.

It's not a restrictive choice to fix the slope (S=1) and to analyse the behaviour of the two bidimensional models already described in presence of a stable density stratification (D=1.1). This is in fact the configuration relevant in practise when dealing with ice flowing on a lower denser layer, represented by frozen compressed till or by liquid water.

The definition of the two basic states follows directly from the sets of equations (42) and (59) previously derived, being for both models:

$$\theta(x,y,t) = \Theta, \qquad \zeta(x,y,t) = Z = 1 - \Theta, \qquad h(x,y,t) = \Theta + Z = 1 \tag{60}$$

and:

$$v(x,y,t) = 0 \tag{61}$$

The longitudinal velocity component is then expressed for the glacier case by:

$$u(x,y,t) = U = R\Theta(Z + D\frac{Z}{2}) \tag{62}$$

while for the ice-shelf one:

$$u(x,y,t) = U = \Theta(Z + D\frac{Z}{2}) \tag{63}$$

Now, since the geometry is unbounded in the y direction and supposed periodic along x, is possible to expand the perturbations from the uniform state for all the variables concerned in the following form:

$$a = A + \tilde{a}(z)exp(ikx + ily + \sigma t) \tag{64}$$

indicating with k and l the longitudinal and trasversal wave numbers of the disturbances and with σ the associated complex eigenvalue. In particular, $Re(\sigma)$ being the growth rate and $Im(\sigma)$ the celerity of the correspondent waves.

Stability conditions are found solving analitically a quadratic algebraic expression in σ and are simply determined by the sign of the real part of the eigenvalue.

The range of unstable wave numbers depends obviously on the choice of the parameters. By fixing $\Theta = 0.5$ (S=1 and D=1.1), it's interesting to note Fig (3) that the sensitivity of the interval of unstable wave numbers on the variations of R appears evident for the glacier model and not for the ice-shelf one.

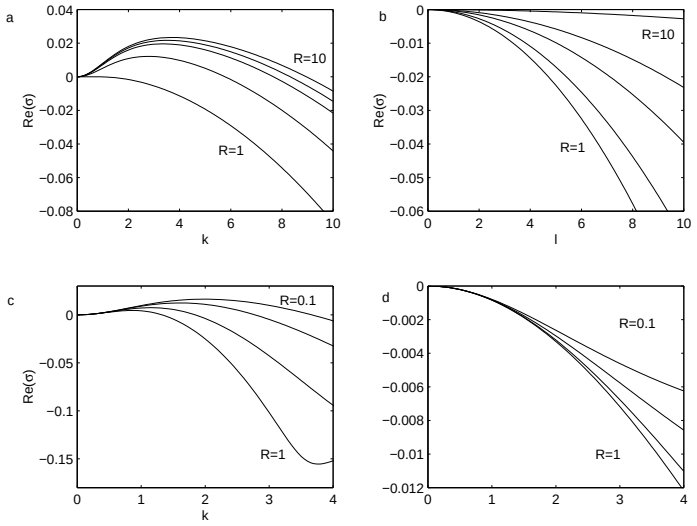

Figure 3: Growth rates as a function of k and l wave numbers, evaluated for increasing values of the parameter R. Curves (a) and (b) show the growth rates for R=1, 2, 5, 10, 100 for the glacier model, while (c) and (d) correspond to R=0.1, 0.2, 0.5, 1 for the ice-shelf approximation.

Two representative solutions of the linear problem are then plotted in Figures (4) and (5).

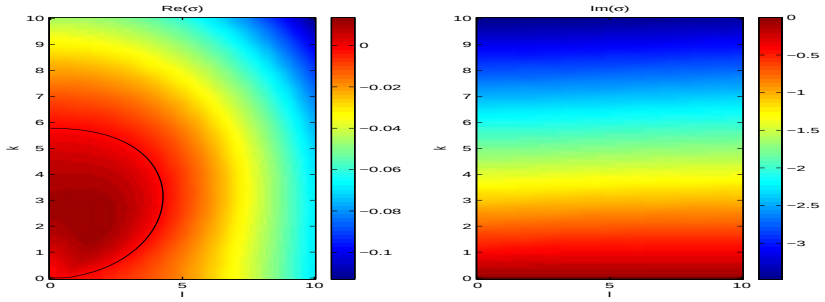

Figure 4: Growth rate $Re(\sigma)$ and phase speed $Im(\sigma)$ in the wave number plane [k,l] for the glacier case, choosen $R = 2$, $\Theta = 0.5$ and $D = 1.1$. The black line in the first plot is the marginal stability curve.

In both cases one can observe the appearance of an instability region in a limited part of the [k,l] plane. The celerities ($c = Im\sigma$) are almost constant along l and show a quite clear linear dependence on k, indicating that all the waves in the plane are moving with the same phase speed ω ($\omega = c/k$).

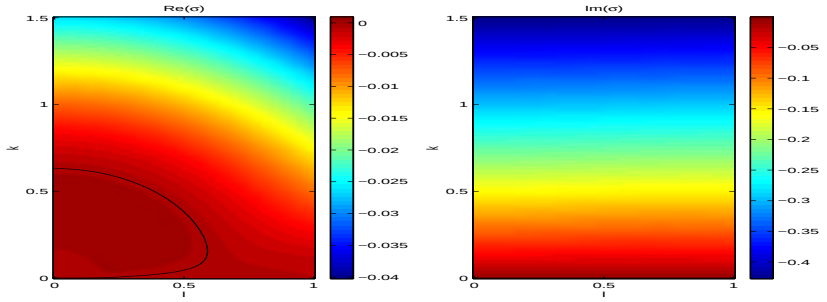

Figure 5: Growth rate $Re(\sigma)$ and phase speed $Im(\sigma)$ in the wave number plane [k,l] in the ice-shelf model with $R = 5$, $\Theta = 0.5$, $D = 1.1$.

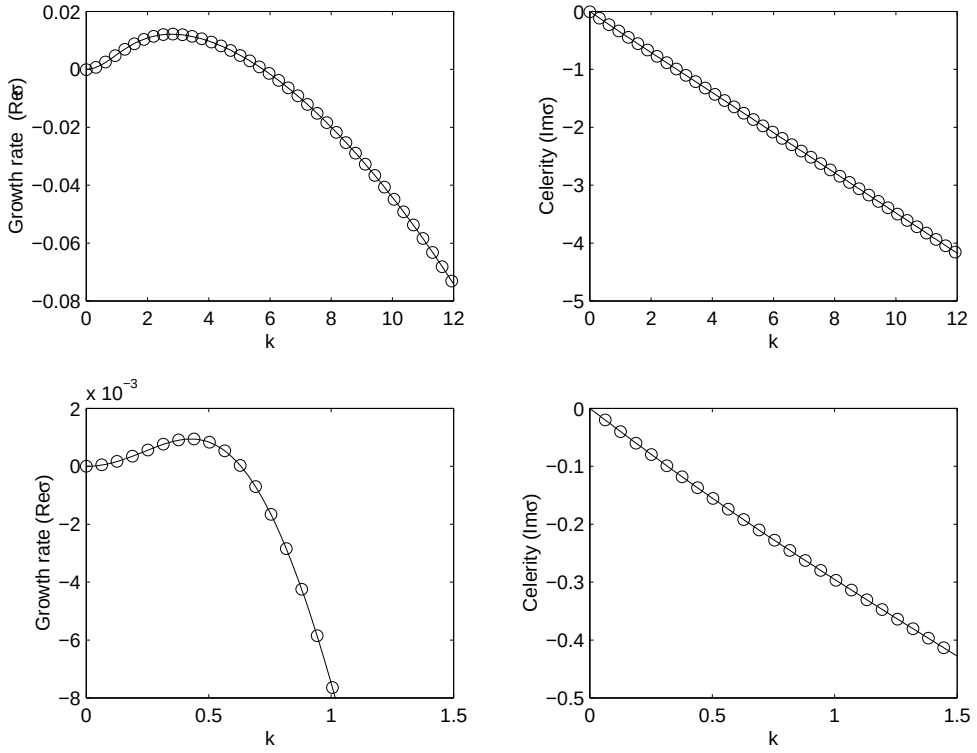

Figure 6: Growth rates and Celerities for a glacier configuration (the upper one, R=2, D=1.1, $\Theta = 0.5$) and for an ice-shelf one (the lower one, R=5, D=1.1, $\Theta = 0.5$) evaluated by the linear theory (solid lines) and by a numerical experiment (circles), running a spectral code with respectively N=128 (Time=500, dt=0.01, Computational domain=20) and N=64 (Time=500, dt=0.002, Computational domain=100) modes.

Figure (6) shows a comparison between the linear theory predictions and numerical experiments performed with the use of a spectral code, displaying a pretty good agreement among theory and simulations.

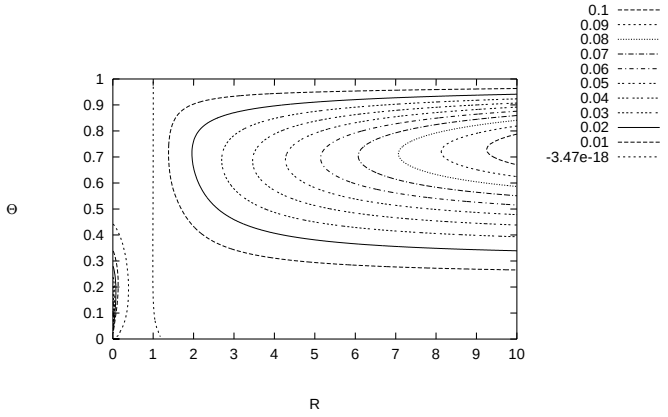

Figure 7: Stability region in the parameter plane $[R, \Theta]$ for S=1, D=1.1 in the glacier case.

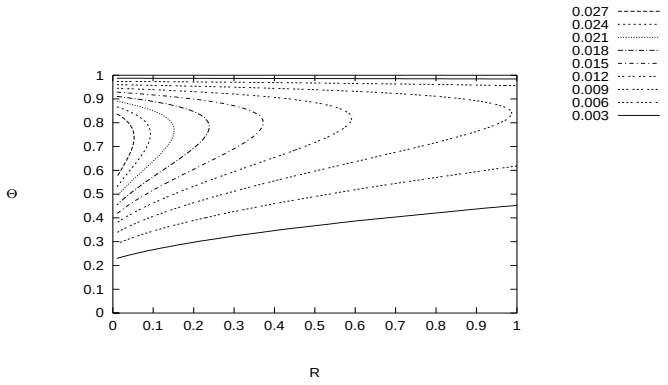

Figure 8: Stability region in the parameter plane $[R, \Theta]$ for S=1, D=1.1 in the ice-shelf case.

Plotting the maximum growth rate in the plane of the parameters R and Θ, is then evident the existence, for the glacier model, of two distinct instability regions (Fig. 7). The first comes out for $R > 1$, no matter the value of Θ, and it's enhanced for increased value of R. The second corresponds to a pretty curious situation with $R \ll 1$ and $\Theta \ll 1$.

In the other model the instability region (Fig.8) covers the whole parameter plane $[\Theta, R]$ and this is in accordance with the interpretation of the ice-shelf approximation as a limit situation for $R = O(\epsilon^{-2}) \gg 1$.

Figure (9) reports then the purely two dimensional instability occurring for values of $R = 0.1, \Theta = 0.2$ in the shear dominated, glacier-like model. A clear explanation of this unespected (at least to the author knowledge) unstable configuration is not available.

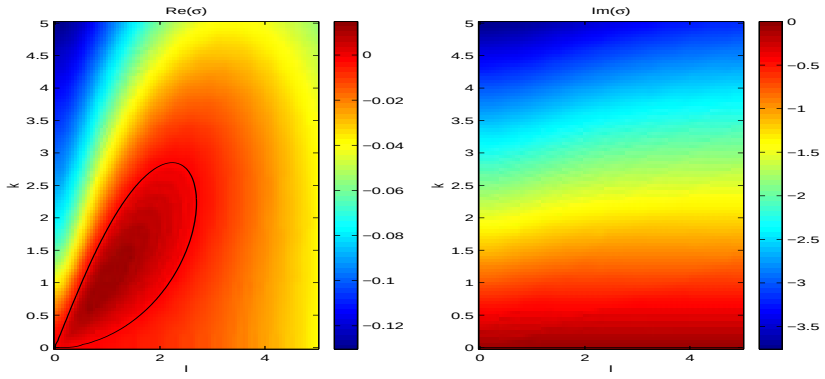

Figure 9: Growth rate $Re(\sigma)$ and phase speed $Im(\sigma)$ in the wave number plane [k,l] for the glacier case, choosen $R = 0.2$, $\Theta = 0.1$ and $D = 1.1$. The black line in the first plot is the marginal stability curve.

The results of such a kind of investigation are interesting, but discouraging to some extent, showing no possibility for fingering to occur.

5.2 Nonlinear dynamic

The governing equations of the two models contain up to fourth order nonlinearities. As a consequence, the evolution of the two interfaces $z = \zeta$ and $z = h$ far away in the future is completely dominated by the nonlinear terms.

The integration in time of the one-dimensional glacier-equations, in a fixed system of reference, is shown in figures (10) and (11).

The initial bump entering the domain at time t=0 moves downstream, growing and evolving as time passes. It's interesting to note the tendence of the system, as time goes on, to sharpen an initially smooth disturbance developing sharp shocks.

The two thicknesses ζ and θ are strongly coupled, oscillating out of phase in time with almost the same amplitude. This means, remembering the physical interpretations of the two, that in a realistic setting one should observe no evolution in time of the free surface.

The same result comes out computing the equilibrium shapes for wave-like solutions of the kind $\theta = \theta(x - ct), \zeta = \zeta(x - ct)$ starting from an initial condition periodic in the spatial domain. Figure (12) displays two equilibrium configurations and a regime diagram indicating the supercritical nature of the bifurcation.

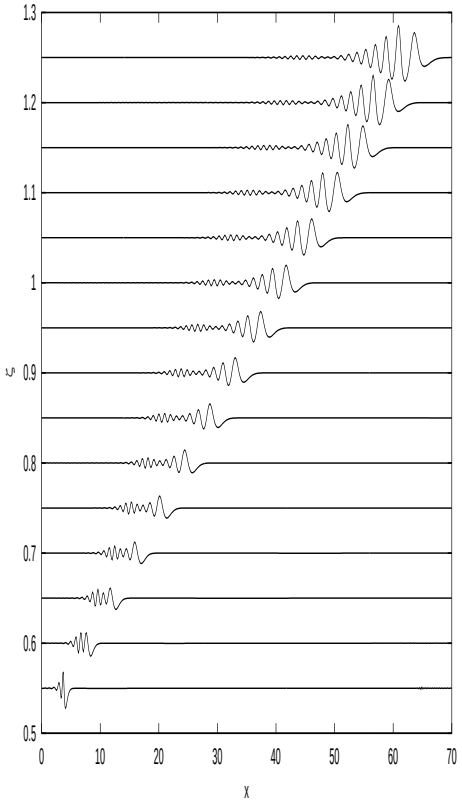

Figure 10: Time evolution of the interface $z = \zeta$ for the glacier case, having fixed $S = 1, D = 1.1, \Theta = 0.5, R = 2$. The system was integrated to time T=500, with time step dt=0.01

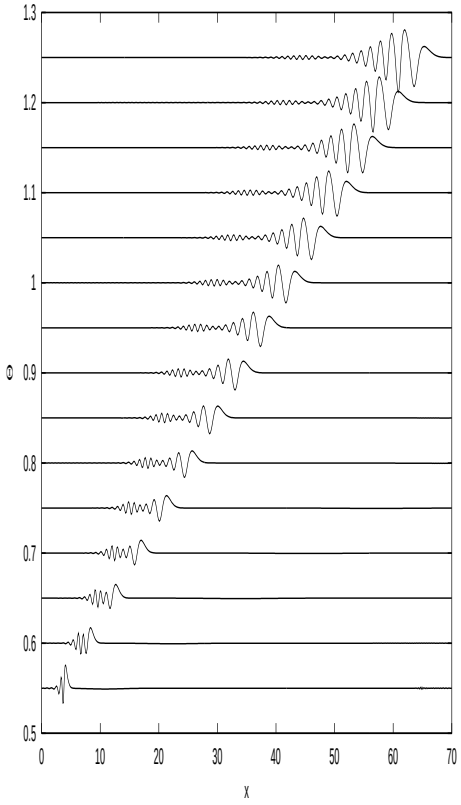

Figure 11: Evolution of $z = \theta$ for the same system. The bump entering the domain from the left is expressed by an exponential law of the form: $F(t) = A * t/t_0 * exp(-t/t_0)$.

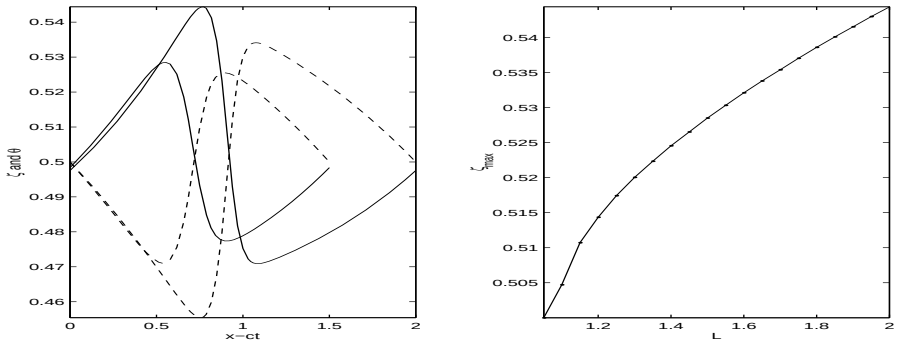

Figure 12: Equilibrium shapes and bifurcation diagram for the glacier model with $S = 1, D = 1.1, R = 2$ and $\Theta = 0.5$. In the plot to the right the solid lines represents the equilibrium shapes of ζ, while the dashed ones describe θ. The couple of solutions correspond to two different choices of the domain lenght, being respectively L=2 and L=1.5

6 The Ice-Stream Model

The models described so far have to do with two furthermost and completely uncorrelated situations, that solely take into account the effects or of the shear stresses (glacier approximation) or of the longitudinal ones (ice-shelf model).

But, to some extent, the behaviour of ice-streams is something in between that ones of glaciers or of ice-shelves. In fact, it becomes rather hazy also in practice to locate the geometric limits of a fast moving ice-stream bounded by an outlet glacier or entering an ice-shelf.

An intermediate model is thus built taking the 1-D non-dimensional set of equations (18) and (19) of the glacier, but without discarding the adjustment produced by the longitudinal stresses on the velocity profile.

The starting point are the followings, describing the system at leading order:

$$\begin{aligned} 0 &= u_{1x} + w_{1z} \\ 0 &= -p_{1x} + \epsilon \partial_x \tau_{xx} + \partial_z \tau_{xz} + S \\ 0 &= -p_{1z} - 1 \end{aligned} \tag{65}$$

$$\begin{aligned} 0 &= u_{2x} + w_{2z} \\ 0 &= -p_{2x} + \partial_z \sigma_{xz} + SD \\ 0 &= -p_{2z} - D \end{aligned} \tag{66}$$

With the usual meaning for the parameters involved, these equations are closed by the set of conditions at the boundaries previously stated.

The longitudinal stresses are expressed by the term $\epsilon \partial_x \tau_{xx}$ in the second of equations (65). It's clear, modeling again the upper fluid as a Newtonian one (and in this case $\tau_{xx} = 2\epsilon\nu_1 u_x$), that this term becomes relevant whenever:

$$\epsilon^2 \nu_1 \sim O(1) \tag{67}$$

This condition is satisfied if $R = \frac{\nu_1}{\nu_2} \gg 1$ and describes a situation in which a much more viscous fluid, characterized by a nearly uniform velocity profile, slides over a less viscous one, with a velocity profile that is parabolic at leading order.

This model is valid for ice-streams since it incorporates the corrections due to longitudinal stresses to a velocity that is not yet completely independent on x.

The next step is the derivation of a consistent and more general thin layer theory, following a procedure analogous to that one described for the glacier. The ice-stream thin layer theory is then expressed by:

$$\begin{aligned} \zeta_t + \partial_x [\frac{1}{2} u\zeta - \frac{1}{12}(DS - \theta_x - D\zeta_x)\zeta^3] &= 0 \\ \theta_t + \partial_x [\theta u + (S - h_x)\frac{\theta^3}{3R}] &= 0 \\ \frac{\zeta^2}{2}(DS - D\zeta_x - \theta_x) + (S - h_x)\theta\zeta + 2\epsilon^2 R\zeta \partial_x(\theta \tau_{xx}) &= u \end{aligned} \tag{68}$$

These equations incorporate two different approximations, reducing to:

- the glacier ones for $R \sim O(1)$;
- the ice-shelf ones for $R \sim O(\epsilon^{-2})$.

7 Conclusions

The purpose of this work was the investigation of two of the mechanisms considered relevant in ice-stream dynamics.

In particular, the extremely simplified models described, were formulated in order to understand the effects on the flow of the different stresses conditions found at the boundary between the flowing ice and its bottom. The explicit treatment of the basal layer, altough complicating the formulation, had the advantage of avoiding strong unphysically grounded assumptions about the structure of the stresses. A second task was, possibly, to relate the action of the stresses to the instability patterns effectively observed in nature.

In this context the glacier and the ice-shelf approximations (the first dominated by shear and the second by longitudinal stresses) were derived and studied. The linear stability analysis revealed the presence of instabilities at the boundaries between the two fluids in both of the models, but showed also the lack of an effective mechanism generating fingers.

Combining the sliding and the slipping properties of the glacier and of the ice-shelf motion, a one-dimensional ice-stream model was then formulated.

These results are far from being relevant for ice, but the analysis can in principle be extended to the consideration of a non Newtonian fluid in motion over a bottom layer, including in the governing equations a different constitutive law.

It could finally be intriguing, for the future, to analyse in more detail the non-linear properties of the models presented, in order to better define their effective capability (or inability) in explaining ice-stream dynamic.

Acknowledgments

I am really greateful to Neil for the long stimulating discussions and for the contagious enthusiasm he was showing when, with the sole help of the chalk, we were fighting on the blackboard against potentially discouraging issues.

I wish then to express my solidariety and admiration to Helen, Fiona, Lianke, Ed, Matt and Taka, that succeeded in bearing me for ten tormented weeks. Thanks for the laughs, the colors, the help and the nice talks.

A lot of people that passed through Walsh Cottage contributed to make it an enjoyable and not conventional environment.

A special mention deserves Shre, that shared my office for all the summer (demonstrating to be extremely patient) and who assisted with me to an impressive number of sunrises, while getting out from the cottage after interminable study sessions.

References

[1] R. B. Alley et al., "Till beneath ice stream B, 3, Till deformation: evidence and implications", J. Geophys. Res., Vol.92 (B9), pp. 8921–8929, 1987

[2] N. J. Balmforth et al., "A consistent thin-layer theory for Bingham plastics", J. Non-Newtonian Fluid Mech., Vol. 84, pp. 65–81, 1999

[3] N. J. Balmforth et al., "Visco-plastic models of isothermal lava domes", J. Fluid Mech., Vol. 403, pp. 37–65, 2000

[4] K. P. Chen, "Wave formation in the gravity-driven low-Reynolds number flow of two liquid films down an inclined plane", Phys. Fluids A, Vol. 5 (12), 3038–3048, 1993

[5] H. Engelhardt et al., "Physical conditions at the base of a fast moving Antartic ice stream", Science, Vol. 248 (4985), pp. 57–59, 1990

[6] A. C. Fowler, "Ice-sheet surging and ice-stream formation", Ann. Glac., Vol. 23, pp 68–73, 1996

[7] T. J. Hughes, Rev. Geophys. Space Phys., Vol. 15, 1977

[8] D. R. MacAyeal, "Large-Scale Ice Flow Over a Viscous Basal Sediment: Theory and Applications to Ice Stream B, Antarctica", J. Geophys. Res., Vol. 94, No. B4, pp. 4071–4087, 1987

[9] D. R. MacAyeal, "The basal stress distribution of Ice Stream E, Antarctica, inferred by control methods", J. Geophys. Res., Vol. 97 (B1), pp. 595–603, 1992

[10] W. S. B. Paterson, *The Physics of Glaciers*, Butterworth-Heinemann, 1998

[11] A. J. Payne, "A Thermomechanical Model of Ice-Flow in West-Antartica", Climate Dynamics, Vol. 15, pp. 115–125, 1999

[12] A. J. Payne, "Dynamics of the siple coast ice stream, West Antartica: results from a thermomechanical ice sheet model", Geophys. Res. Lett., Vol. 25 (16), pp. 3173–3176, 1998

[13] C. Pozrikidis, "Gravity-driven creeping flow of two adjacent layers through a channel and down a plane wall", J. Fluid Mech., Vol. 371, pp. 345–376, 1998

[14] B. S. Tilley et al., "Linear stability theory of two-layer fluid flow in an inclined channel", Phys. Fluids, Vol. 6 (12), pp.3906–3922, 1994

[15] S. J. Weinstein, "Large growth instabilities in three-layer flow down an incline in the limit of zero wave Reynolds wave number", Phys. Fluids, Vol. 11 (11), 3270–3282, 1999